Journal of Alloys and Compounds 506 (2010) 224–230

Contents lists available at ScienceDirect

Journal of Alloys and Compounds

journal homepage: www.elsevier.com/locate/jallcom

Mechanochemically driven nonequilibrium processes in MNH_2–CaH_2 systems (M = Li or Na)

Oleksandr Dolotko[a,b], Haiqiao Zhang[a,b], Sa Li[c], Puru Jena[c], Vitalij Pecharsky[a,b,*]

[a] Ames Laboratory, US Department of Energy, Iowa State University, Ames, IA 50011-3020, USA
[b] Department of Materials Science and Engineering, Iowa State University, Ames, IA 50011-2030, USA
[c] Department of Physics, Virginia Commonwealth University, Richmond, VA 23284, USA

ARTICLE INFO

Article history:
Received 1 March 2010
Accepted 29 June 2010
Available online 7 July 2010

Keywords:
Hydrides
Hydrogen storage
Mechanical milling
Density functional theory

ABSTRACT

Mechanochemical transformations of lithium and sodium amides with calcium hydride have been investigated using gas volumetric analysis, X-ray powder diffraction, and residual gas analysis. The overall mechanochemical transformations are equimolar, and they proceed as the following solid state reaction: $MNH_2 + CaH_2 \rightarrow CaNH + MH + H_2$, where M = Li or Na. The transformation kinetics of the lithium containing system is markedly faster compared to the system with sodium. The difference in the rates of solid state transformations, and therefore, in hydrogen release kinetics can be explained by difference in mobility of lithium and sodium atoms. Total energies and enthalpies of formation for different reaction products during the dehydrogenation of CaH_2–MNH_2 mixtures were calculated using density functional theory. Compared to thermochemical transformations, which proceed in accordance with thermodynamic equilibrium, reactions induced by mechanical energy drive the MNH_2–CaH_2 systems to nonequilibrium configurations with different final products.

1. Introduction

Related to the need for high capacity hydrogen storage materials there is a growing interest in lightweight compounds such as lithium- and sodium-based hydrides. Among them, metal–nitrogen–hydrogen (M–N–H) systems have been regarded as one of the most attractive hydrogen storage materials. Recently, Chen et al. [1] reported that hydrogenation and dehydrogenation of lithium nitride can be performed *via* the following reversible two-step reaction:

$$Li_3N + 2H_2 \overset{195\,^\circ C;\,0.2\,bar}{\longrightarrow} Li_2NH + LiH + H_2 \underset{280^\circ C;\,1\,bar}{\overset{255\,^\circ C;\,1.5\,bar}{\longleftrightarrow}} LiNH_2 + 2LiH \quad (1)$$

Theoretically, as much as 10.4 wt.% of hydrogen can be stored using this system. Since the second step of this reaction is characterized by a small enthalpy change, 5.2 wt.% of hydrogen is reversible. Yet, many material-related problems prevent immediate use of lithium nitride as hydrogen storage material, one of which is the high dehydrogenation temperature.

In order to improve Li_3N as a hydrogen storage material, some work has been performed to destabilize Li–N–H system by adding Ti catalyst [2,3] or other hydrides. Much of the recent effort has been focused on overcoming both the thermodynamic and kinetic barriers, associated with the $LiNH_2$/LiH system. A particularly interesting approach was suggested by Luo [4] and by Xiong et al. [5] who lowered the hydrogen desorption temperature by substituting LiH with MgH_2. This substitution decreases the hydrogen desorption temperature (extrapolated to 1 bar hydrogen atmosphere) [4] from 280 °C in Li–N–H to 80 °C in Mg–Li–N–H *via* the following reaction:

$$2LiNH_2 + MgH_2 \rightarrow Li_2Mg(NH)_2 + 2H_2 \quad (2)$$

The hydrogen storage properties of the Li–Mg–N–H system have been investigated using thermal decomposition [6–9] and mechanical milling [10–12]. It was shown that after the initial dehydrogenation reaction (2) between $LiNH_2$ and MgH_2 taken in a 2:1 molar ratio, which leads to the formation of $Li_2Mg(NH)_2$, the product can be rehydrogenated forming $Mg(NH_2)_2$/LiH mixture. Therefore, the reversible sorption process is between $Li_2Mg(NH)_2 + 2H_2$ and $Mg(NH_2)_2 + 2LiH$ as described in (3):

$$2LiNH_2 + MgH_2 \rightarrow Li_2Mg(NH)_2 + 2H_2 \leftrightarrow Mg(NH_2)_2 + 2LiH \quad (3)$$

Groups 1, 2, 13 and 14 elements easily form nitrides, hydrides, amides or imides. Thus, it is possible to design numerous metal–N–H systems with reactions similar to (1), which may or may not be suitable for hydrogen storage applications but must be

* Corresponding author at: Ames Laboratory, Department of Materials Science and Engineering, Iowa State University, Ames, IA 50011-3020, USA.
Tel.: +1 515 294 8220; fax: +1 515 294 9579.
E-mail address: vitkp@ameslab.gov (V. Pecharsky).

0925-8388/$ – see front matter © 2010 Elsevier B.V. All rights reserved.
doi:10.1016/j.jallcom.2010.06.181

studied to gain basic insights on the phase transformation mechanisms. For instance, Luo [4] and Xiong e al. [5] demonstrated that binary systems such as $Mg(NH_2)_2$–2LiH and $LiNH_2$–CaH_2 exhibit high hydrogen storage capacity with improved thermodynamics. Xiong [5] and Wu et al. [13] reported that hydrogen absorption–desorption characteristics and final products of interaction in Li–Mg–N–H and Li–Ca–N–H systems are similar. For example, $Li_2Ca(NH)_2$ ternary imide was successfully synthesized by dehydrogenating a mixture of $LiNH_2$ and CaH_2 taken in a 2:1 molar ratio using a synthetic route similar to (2) [13]. Hydrogen storage properties of the Li–Ca–N–H system were recently examined by Tokoyoda et al. [14]. They prepared two kinds of mixtures: $Ca(NH_2)_2$–2LiH and CaH_2–2$LiNH_2$ that were ball milled for 2 h, and their hydrogen desorption and absorption characteristics were examined by thermal desorption and mass spectroscopy combined with thermogravimetry and differential thermal analysis. Both composites form Li_2NH and CaNH compounds after dehydrogenation at 200 °C; both systems were transformed into an "unknown imide phase" after heating to 400 °C. Authors of Ref. [14] concluded that the overall reversible reaction in the Li–Ca–N–H system can be expressed as (4), and that the hydrogen capacity is 4.5 wt.%:

$$CaH_2 + 2LiNH_2 \rightarrow CaNH + Li_2NH + 2H_2 \leftrightarrow Ca(NH_2)_2 + 2LiH \quad (4)$$

The "unknown imide phase", which forms after 400 °C, is $Li_2Ca(NH)_2$ ternary imide isolated and characterized by Wu et al. [13]. Recently, Ca–Na–N–H system was evaluated by Xiong et al. [15]. Similar to other amide–hydride systems, interaction between $Ca(NH_2)_2$ and NaH (1:1) was observed in the temperature range of 120–270 °C with 1.1 wt.% of hydrogen desorbed, of which 0.96 wt.% of hydrogen can be recharged.

Building upon our previous research, in which we showed that ball milling may be an excellent tool to rapidly destabilize a complex hydride system and may lead to an array of solid state reactions [16], here we investigate room temperature mechanochemical reactions between MNH_2 (M = Li, Na) and CaH_2 taken in different molar ratios. Even though ball milling is a common technique employed to mix solid hydride phases for further investigations of their thermochemical behaviors, it is also a very convenient and effective, yet an underappreciated tool to conduct solid state reactions. As we will show below the mechanisms of mechanochemical transformations of the same system may be different from those induced by temperature.

Furthermore, existence of several calcium nitrides, amides and imides, such as Ca_3N_2 [17,18], Ca_2N [19–22], CaNH [23], Ca_2NH [24,25], and $Ca(NH_2)_2$ [26–28] prompted us to also investigate mixtures in molar ratios from which the corresponding compounds may be produced from CaH_2 and MNH_2. Thus, to obtain Ca_3N_2 a 3:2 molar ratio of the components is required, for CaNH it becomes 1:1, Ca_2NH and Ca_2N 2:1, and for $Ca(NH_2)_2$ a 1:2 mixture of CaH_2 and MNH_2 is needed.

2. Experimental details

The starting materials $LiNH_2$ (95 wt.% purity), $NaNH_2$ (>90 wt.% purity) and CaH_2 powder (90–95 wt.% purity) were purchased from Sigma–Aldrich. Mixtures of the alkali metal amides with calcium hydride taken in different molar ratios (~1 g of mixture total) were loaded in a 50 ml hardened steel vial and ball milled using 20 g of steel balls (two large balls weighing 8 g each and four small balls weighing 1 g each) in an 8000M SPEX mill. The ball milling was stopped at different time intervals and phase analysis of the mixture was carried out.

For the gas volumetric measurements after the ball milling, a magnetic ball mill "Uni-Ball-Mill 5" was used. Mixtures of hydrides were ball milled in a 90 ml hardened steel vial, equipped with a gas outlet port. During the ball milling of ~3 g of hydride mixture, 179.6 g steel balls were used (8 balls weighing 16 g each, 4 balls weighing 8 g each, 5 balls weighing 3.5 g each and 15 balls weighing 0.14 g each). Pressure changes were measured by connecting the vial to the PCTPro 2000 system after the mechanochemical treatment. Volume calibration was performed at room temperature before the ball milling. The RGA-100 residual gas analyzer was used for the qualitative analysis of the released gas.

Solid reaction products were characterized by X-ray powder diffraction at room temperature on a Scintag powder diffractometer using Cu Kα radiation, in the range of Bragg angles 2θ from 10° to 80°. The measurements were performed using a sample holder, covered by two kinds of thin plastic films, used to protect the sample from air. One of the films produces an amorphous-like background between 13° and 18° of 2θ and another film produces broad halos in the region between 15° and 23° of 2θ. Due to air sensitivity of the starting materials and the products, all manipulations have been carried out in argon atmosphere in a glove box.

3. Thermodynamic analyses

3.1. Computation procedure

To gain an insight on the stability of the intermediate phases that could form during mechanochemical transformations of lithium and sodium amides with calcium hydride, taken in 1:1 and 2:1 molar ratios, we have calculated the crystal parameters, electronic structure, total energies, and the enthalpy of formation of a wide range of hydrides [CaH_2, CaNH, $Ca(NH_2)_2$, $LiNH_2$, Li_2NH, LiH, $Li_2Ca(NH)_2$, $NaNH_2$, Na_2NH, NaH and $Na_2Ca(NH)_2$]. Total energy and geometry optimization calculations were carried out using density functional theory (DFT) [29] and generalized gradient approximation (GGA) [30] for exchange and correlation potentials. The calculations were performed using Vienna *ab initio* simulation package (VASP) [31] and the projector augmented wave (PAW) [32] method. High precision calculations with a cutoff energy of 500 eV for the plane-wave basis were performed. The equilibrium crystal structures and lattice parameters were obtained by starting with initial structures given by existing experiments and optimizing the geometries without any symmetry constraints. In all calculations, self-consistency was achieved with a tolerance in the total energy of at least 0.1 meV.

3.2. Crystal structure

Among the above-mentioned compounds, $LiNH_2$ has been well studied. It has a tetragonal structure and belongs to space group symmetry $I\bar{4}$. The structure was determined experimentally [33] and detailed calculations can be found in Refs. [34–36]. For Li_2NH, we have used the Li_2ND (orthorhombic *Ima2*) as the starting structure [35]. Our calculated parameters given in Table 1 agree well with those of Herbst and Hector [35]. We considered two structures for $NaNH_2$; the first one has lithium amide tetragonal structure (space group $I\bar{4}$), while the other one is orthorhombic (space group *Fddd*) [37,38]. Our calculations show that the orthorhombic structure is the ground state for $NaNH_2$. For Na_2NH, which is not found experimentally, the Li_2NH structure as the input geometry was used.

There are several possible products or intermediate phases that can form during the dehydrogentaion of lithium (sodium) amide and calcium hydride mixture. These are: CaNH, $Ca(NH_2)_2$, $Li_2Ca(NH)_2$ and $Na_2Ca(NH_2)_2$. To obtain the ground state geometry of the CaNH crystal, we used two initial structures. One is reported by Sichla and Jacobs [23], which is a face centered cubic (*fcc*) structure with space group $Fm\bar{3}m$, $Z = 4$, $a = 5.143$ Å. The other, taken from the work of Wegner et al. [39], is a BaND structure hav-

Table 1
Crystal structures of compounds, used for thermodynamic calculations. The space group, number of the space group, Z (number of molecules per unit cell), relaxed lattice parameters (a, b, c (Å), α, β, and γ (°)), and energy per molecule (eV per formula unit).

Compound	Space group	Z	a	b	c	α	β	γ	E (mol)
CaH_2 [43]	*Pnma*	4	5.929	3.582	6.795	90	90	90	−10.494
CaNH [23]	*P*1	4	5.132	5.298	5.177	83.7	90	90	−16.115
CaNH (BaND) [39]	*P*1	2	3.515	3.805	5.169	90	96.8	90	−16.116
$Ca(NH_2)_2$ (224) [27,40]	$I4_1/acd$	32	10.665	10.665	21.031	90	90	90	−36.153
$Ca(NH_2)_2$ (28) [41]	$I4_1/amd$	4	5.076	5.076	10.308	90	90	90	−36.612
$LiNH_2$ [33]	$I\bar{4}$	8	4.993	4.993	10.331	90	90	90	−19.153
Li_2NH [35]	*Ima*2	16	7.128	10.080	7.095	90	90	90	−17.638
LiH [46]	$Fm\bar{3}m$	4	4.007	4.007	4.007	90	90	90	−6.171
$Li_2Ca(NH)_2$ (2d) [13]	$P\bar{3}m1$	1	3.840	3.840	5.361	90	90	120	−33.365
$Li_2Ca(NH)_2$ (6i) [42]	*P*1	1	3.702	3.702	5.888	93.5	86.5	121.2	−33.584
$NaNH_2$ [37,38]	*Fddd*	16	8.941	10.466	8.089	90	90	90	−17.983
$NaNH_2$	$I\bar{4}$	8	5.804	5.804	11.487	90	90	90	−17.958
Na_2NH	*Ima*2	16	8.511	11.954	8.343	90	90	90	−14.949
NaH	$Fm\bar{3}m$	4	4.817	4.817	4.817	90	90	90	−5.153
$Na_2Ca(NH)_2$ (2d)	$P\bar{3}m1$	1	4.049	4.049	5.937	90	90	120	−30.805
$Na_2Ca(NH)_2$ (6i)	*P*1	1	3.931	3.931	6.943	97.9	82.0	119.5	−30.796

ing tetragonal symmetry and either $I4/mmm$ or $I\bar{4}m2$ space group with $a = 4.062$ Å, $c = 6.072$ Å and $Z = 2$. Since H atoms only partially occupy the Wyckoff 24*e* positions in the $Fm\bar{3}m$ space group, we performed two calculations with and without the *fcc* symmetry. In the first one, we kept the *fcc* Bravais lattice where there are only three atoms in the primitive unit cell ($Z = 1$). The sites of these three atoms are Ca (0, 0, 0), N (0.5, 0.5, 0.5) and H (0.35, 0.35, −0.35) [23]. In the second calculation, we used a primitive cubic Bravais lattice ($Z = 4$). We optimized the geometry by totally breaking the symmetry of the *fcc* lattice (assuming *P*1 space group symmetry) and positioning the hydrogen atoms at a distance given by the experimental N–H distance.

Similar procedure (one with body centered tetragonal (*bct*) symmetry and the other one without) was adopted for the BaND-like structure where only two N atoms and two H atoms occupy Wyckoff 4*a* and 16*n* sites, respectively. By comparing total energy of the relaxed structures, we found that both structures with *P*1 symmetry are lower in energy than the corresponding structures with symmetry constraints. It does not matter whether one starts from CaNH (*fcc*) or BaND (tetragonal) like structure, but once the symmetry group is reduced to *P*1, both lead to the same energy, namely, 16.115 and 16.116 eV/molecule.

For $Ca(NH_2)_2$, we included both $Ca(NH_2)_2$-like [27,40] and $Mg(NH_2)_2$-like [41] structures as our starting configurations. $Ca(NH_2)_2$ is tetragonal with the space group $I4_1/amd$. The sites for Ca, N, and D atoms are respectively 4*a* (0 ¾ $^1/_8$), 8*e* (0 ¼ 0.115) and 16*h* (0.158 ¼ 0.160). $Mg(NH_2)_2$ has the space group $I4_1/acd$ with $a = 10.3758$ Å and $c = 20.062$ Å, and its unit cell consists of 224 atoms ($Z = 32$). Our results show that the tetragonal structure with space group $I4_1/amd$ is 0.46 eV lower in energy than the one belonging to $I4_1/acd$ space group.

Even though the crystal structure of $Li_2Ca(NH)_2$ has been determined, the positions of H atoms remain unresolved due to the limitations of the X-ray diffraction method [13]. According to the symmetry of $P\bar{3}m1$ space group, H atoms can either occupy Wyckoff 2*d* positions or partially occupy 6*i* positions. Through first principles calculations, Bhattacharya et al. [42] pointed out that H prefers 6*i* over 2*d* positions. Our results are in agreement with their calculations; partial occupation of 6*i* position lowers the energy by 0.2 eV. However, as we observed for the CaNH structure, because of the partial occupancy of the 6*i* sites the symmetry is lowered to *P*1. In contrast, H atoms prefer the 2*d* site in $Na_2Ca(NH)_2$. Hence, $Na_2Ca(NH)_2$, which is not discovered experimentally, can be trigonal and belong to $P\bar{3}m1$ space group.

We used standard structures for CaH_2 (*Pnma*, $a = 5.925$ Å, $b = 3.581$ Å and $c = 6.776$ Å) [43–45], LiH ($Fm\bar{3}m$, $a = 4.066$ Å) [46] and NaH ($Fm\bar{3}m$, $a = 4.88$ Å) [47] as input structures. The relaxed lattice parameters are listed in Table 1.

4. Results and discussion

4.1. Mechanochemical transformations

4.1.1. MNH_2–CaH_2 (1:1) system, M = Li or Na

A mixture of $NaNH_2$ and CaH_2 hydrides taken in a 1:1 molar ratio was ball milled for 1, 3, 5, 7, 9 and 24 h, and progression of the transformation was followed by X-ray powder diffraction analysis. The X-ray patterns of the mixture before and after different ball milling times are shown in Fig. 1. Considerable changes in the mixture were observed between 0 and 7 h but after that the changes become minimal and after the 9 h the X-ray pattern does not change. Hence, it appears that the reaction is completed and 9 h of ball milling is enough to finish this solid state transformation.

The same approach was used to study mechanochemical transformation in the mixture of $LiNH_2$ and CaH_2 hydrides taken in a 1:1 molar ratio. According to X-ray diffraction analysis (Fig. 2), a solid state reaction in this system is completed after 7 h of ball milling.

As follows from Fig. 1, when the transformation is complete there are two poorly crystalline products in the system. The first is calcium imide – CaNH – which has a cubic crystal structure (space group $Fm\bar{3}m$, $a = 5.143$ Å). The same compound is also a

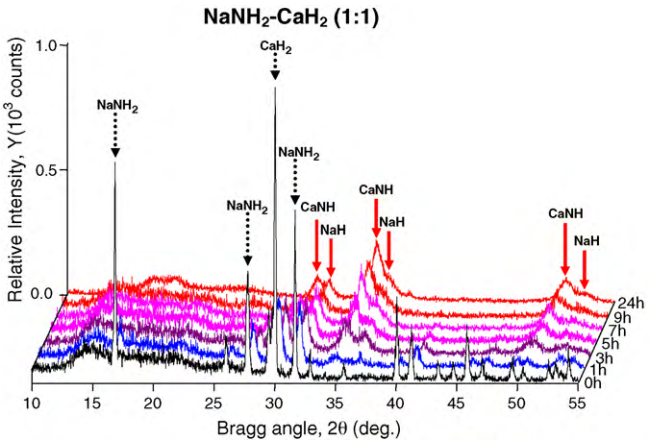

Fig. 1. The X-ray powder diffraction patterns of the physical mixture of $NaNH_2 + CaH_2$ taken in a 1:1 molar ratio and of the same measured after different ball milling times.

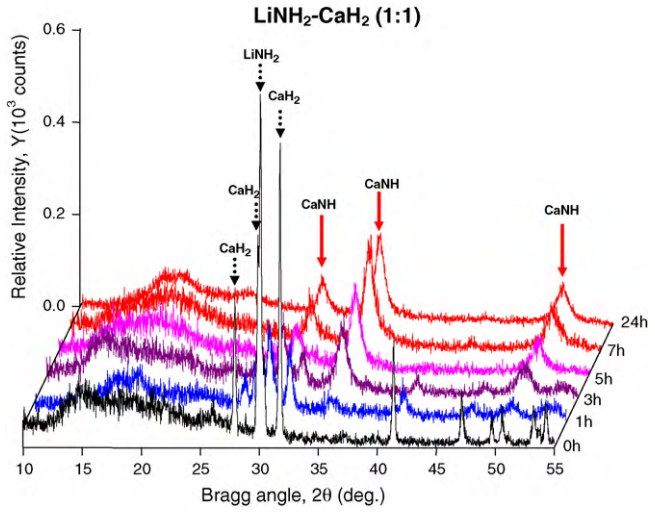

Fig. 2. The X-ray powder diffraction patterns of the physical mixture of $LiNH_2 + CaH_2$ taken in a 1:1 molar ratio and of the same measured after different ball milling times.

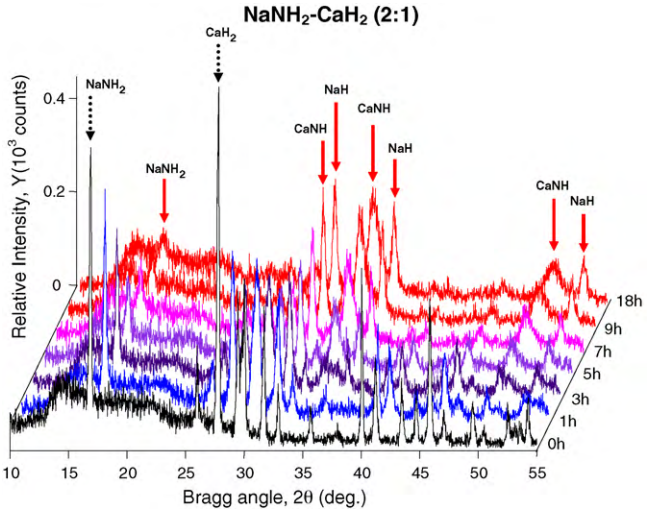

Fig. 3. The X-ray powder diffraction patterns of the physical mixture of $NaNH_2 + CaH_2$ taken in a 2:1 molar ratio and of the same measured after different ball milling times.

major crystalline component of the product after ball milling of the $LiNH_2$–CaH_2 system (Fig. 2). The crystal structure of calcium imide obtained mechanochemically corresponds to that described by Sichla and Jacobs [23]. Another solid product of the reaction in the $NaNH_2$–CaH_2 system is sodium hydride – NaH. Bragg peaks of LiH are impossible to distinguish in Fig. 2, which is due to a combination of the low scattering ability of Li and H and a poor crystallinity after a prolonged milling [16]. Considering that one product (CaNH) is identical in both systems, LiH does indeed form in the $LiNH_2$–CaH_2 system.

Similar difficulties with detecting LiH by X-ray analysis after mechanochemical processing were noted in our previous work [16], where we employed ^{7}Li solid state nuclear magnetic resonance to prove the presence of LiH. It was also shown that in all similar light metal systems, formation of NaH when M is sodium is a solid indicator that LiH forms in an analogous lithium system. Considering also high thermodynamic stability of LiH and NaH this makes the formation of LiH in the $LiNH_2$–CaH_2 system highly feasible even though lithium monohydride cannot be positively identified in Fig. 2 from X-ray powder diffraction data.

Another proof of the identical stoichiometry in the reactions in both lithium and sodium systems was obtained from gas volumetric analysis. After milling of the $LiNH_2$–CaH_2 system in a magnetic ball mill for 216 h, hydrogen is released in an equimolar quantity, i.e. one-half of the available hydrogen is obtained. The same equimolar quantity of the hydrogen has been released from the $NaNH_2$–CaH_2 system ball milled for 236 h. The time necessary to complete both reactions using the magnetic ball mill was established by comparing the X-ray powder patterns of the mixtures ball milled for different time intervals. The composition analysis of the gas formed in the vial after ball milling reveals emission of the pure hydrogen in both systems. No other gases were detected by residual gas analysis.

Taking into account the results of X-ray powder diffraction, gas volumetric and residual gas analyses we conclude that the overall mechanochemical transformations in the $NaNH_2$–CaH_2 system taken in a 1:1 molar ratio proceeds according to (5), and that in the $LiNH_2$–CaH_2 mixture according to (6).

$$NaNH_2 + CaH_2 \rightarrow CaNH + NaH + H_2, \quad [\sim 2.5\,wt.\%\,H_2] \qquad (5)$$

$$LiNH_2 + CaH_2 \rightarrow CaNH + LiH + H_2, \quad [\sim 3.1\,wt.\%\,H_2] \qquad (6)$$

4.1.2. MNH_2–CaH_2 (2:1) system, M = Li or Na

This stoichiometry was examined in order to verify whether or not $Ca(NH_2)_2$ or $Li_2Ca(NH)_2$ compounds can be prepared using mechanochemistry. The X-ray powder patterns in the $2NaNH_2$–CaH_2 system change with ball milling up to 9 h. After this no further changes were observed. Calcium imide, sodium hydride and excess of sodium amide were found as end solid products of this interaction (Fig. 3).

Transformations occurring in the $2LiNH_2$–CaH_2 system are similar and reaction is completed after 7 h of ball milling (Fig. 4). Once again, there are difficulties with identification of lithium compounds in the reaction mixture. Lithium hydride, LiH, is likely to form since NaH does form in the $NaNH_2$–CaH_2 (2:1) system.

Another difficulty is in differentiating between the newly formed CaNH and Li_2NH imides and the excess of $LiNH_2$ amide. Since Bragg peaks that belong to CaNH are located close to those of $LiNH_2$ and Li_2NH, it is difficult to unquestionably detect either $LiNH_2$ or Li_2NH after the processing. Formation of the Li_2NH compound in a mixture is possible if excess $LiNH_2$ will react with the formed LiH ($LiNH_2 + LiH \rightarrow Li_2NH + H_2$). To check the possibility of this reaction, a mixture of LiH and $LiNH_2$ taken in a 1:1 molar ratio was ball milled for 7 h. X-ray powder diffraction characterization of

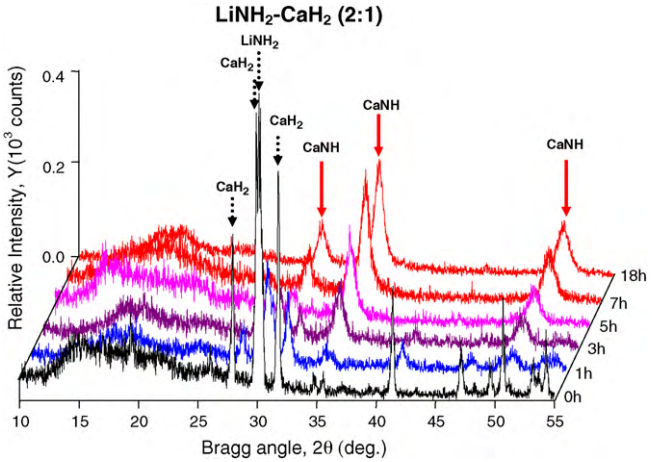

Fig. 4. The X-ray powder diffraction patterns of the physical mixture of $LiNH_2 + CaH_2$ taken in a 2:1 molar ratio and of the same measured after different ball milling times.

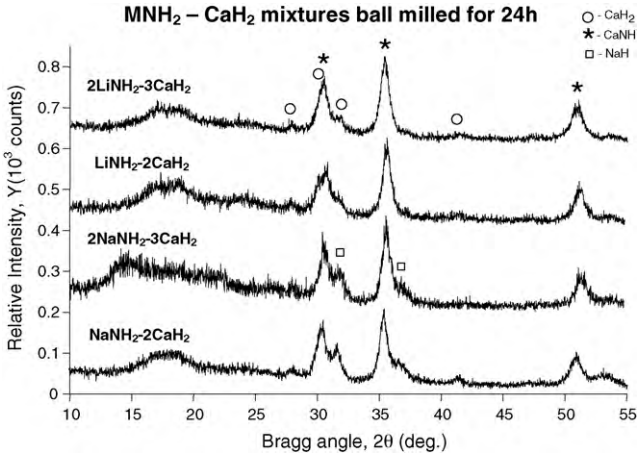

Fig. 5. The X-ray powder diffraction patterns of $MNH_2 + CaH_2$ mixtures taken in a 1:2 and 2:3 molar ratios ball milled for 24 h.

the ball milled sample shows only starting materials and, therefore, there is no solid state reaction between lithium imide and lithium hydride during mechanochemical treatment. Taking into account all of the above, we may conclude that calcium imide, lithium hydride and excess of lithium amide are present in a $2LiNH_2$–CaH_2 mixture after its dehydrogenation transformation by ball milling.

Hence, mechanochemical dehydrogenation reactions in $2MNH_2$–CaH_2 systems proceed according to (5) and (6) with the formation of CaNH, light metal hydride, gaseous hydrogen and excess of MNH_2 in a mixture. Finally, $Ca(NH_2)_2$ or $Li_2Ca(NH)_2$ compounds do not form as the final products of these reactions, even though stoichiometry of the systems is suited for these two types of compounds.

4.1.3. MNH_2–CaH_2 (1:2) and (2:3) systems, M = Na or Li

In an attempt to reach a more complete dehydrogenation of MNH_2–CaH_2 systems with formation of Ca_2N, Ca_2NH or Ca_3N_2 compounds, mixtures of light metal amides and calcium hydride taken in a 1:2 and 2:3 molar ratios of components were ball milled for 24 h. After phase analyses of the products it is easy to conclude, that in all four cases CaNH, alkali metal monohydride MH and excess CaH_2 are present (Fig. 5). Hence, Ca_2N and Ca_2NH do not form after mechanochemical treatment of MNH_2–$2CaH_2$ mixtures; Ca_3N_2 was not synthesized by ball milling of the $2MNH_2$–$3CaH_2$ systems. Similar to other stoichiometries described above, solid state interactions occur according to reactions (5) and (6) with the nonreacted CaH_2 phase remaining in a mixture even after a prolonged milling.

4.2. Thermodynamic analysis

Thermodynamic analysis was performed by calculating total energies and enthalpies of formation of related structures listed in Table 1. The energy of an H_2 molecule is calculated to be 6.8 eV, but it is reduced to 4.581 eV once the atomic energy of H is corrected by using the spin polarization formalism. However, in computing the enthalpy of formation during various reactions, this correction is not important: the atomic energies of H cancel out as both the reactants and reaction products contain the same number of H atoms.

The enthalpies of formation in various possible reactions are listed in Table 2. We have considered four feasible reaction paths for both CaH_2–$LiNH_2$ and CaH_2–$NaNH_2$ systems. The reaction paths marked 1–3 are one-step reactions and that marked 4 is a two-step reaction. We see that all reactions are endothermic except for the reaction $CaH_2 + 2LiNH_2 \rightarrow Ca(NH_2)_2 + 2LiH$ (path marked 4 in Table 2). It is actually exothermic with enthalpy of formation of 14.9 kJ/mol (0.155 eV). We also note that Tokoyoda et al. [14] observed that after rehydrogenation of the dehydrogenated products of $Ca(NH_2)_2$–2LiH and CaH_2–$2LiNH_2$ mixtures, both products were observed experimentally to transform into mixtures of $Ca(NH_2)_2$–2LiH. This demonstrates that $Ca(NH_2)_2$–2LiH mixture is more stable than CaH_2–$2LiNH_2$ and also validates our computed results.

We also calculated the enthalpy of formation for the reaction $Ca(NH_2)_2 + 2LiH \rightarrow CaNH + Li_2NH + 2H_2$. The reaction is endothermic with a heat of formation of 77 KJ/mol/H_2. Since the heat of formation for the reaction $CaH_2 + LiNH_2 \rightarrow CaNH + Li_2NH + H_2$ is 70 KJ/mol/H_2, $CaH_2 + 2LiNH_2$ composite should require lower temperature for dehydrogenation than $Ca(NH_2)_2 + 2LiH$ mixture. This is indeed what was observed by Tokoyoda et al. [14], namely hydrogen desorption took place at 200 and 220 °C for the $CaH_2 + 2LiNH_2$ and $Ca(NH_2)_2 + 2LiH$ composites, respectively. At a temperature of 400 °C, an unknown imide phase was identified to be $Li_2Ca(NH)_2$ [40]. We see from the enthalpy of formation in step 2A and step 2B in path 4 in Table 2 that it costs more energy to form $Li_2Ca(NH)_2$ than CaNH–Li_2NH mixture. This is why CaNH–Li_2NH mixture was observed at 200 °C, but $Li_2Ca(NH)_2$ phase was only observed at 400 °C.

For the Na-based system, the reaction, $CaH_2 + 2NaNH_2 \rightarrow Ca(NH_2)_2 + 2NaH$, is also exothermic and accompanied by energy release of 44.2 kJ/mol (0.458 eV). The above heat of formation shows that dehydrogenation from $CaH_2 + 2NaNH_2$ mixture is also a two-step process, with $Ca(NH_2)_2$ being an intermediate phase.

However, $Ca(NH_2)_2$ phase was not observed in the reaction products in the present experiment. The discrepancy between the present experiment and that of Tokoyoda et al. [14] is due to the experimental temperature. We note that the experiment by Tokoyoda et al. [14] was carried out up to 400 °C, while the present

Table 2
Enthalpies of formation for different reaction products during the dehydrogenation of CaH_2 and $LiNH_2$ (or $NaNH_2$) mixture.

Reactants	Path	Reaction products	ΔE (eV)	ΔH (kJ/mol/H_2)
$CaH_2 + LiNH_2$	1	$CaH_2 + LiNH_2 = CaNH + LiH + H_2$	0.560	54.032
	2	$CaH_2 + 2LiNH_2 = Li_2Ca(NH)_2 + 2H_2$	1.615	77.912
	3	$CaH_2 + 2LiNH_2 = CaNH + Li_2NH + 2H_2$	1.445	69.711
	4	Step 1: $CaH_2 + 2LiNH_2 = Ca(NH_2)_2 + 2LiH$	−0.155	
		Step 2A: $Ca(NH_2)_2 + 2LiH = CaNH + Li_2NH + 2H_2$	1.600	77.188
		Step 2B: $Ca(NH_2)_2 + 2LiH = Li_2Ca(NH)_2 + 2H_2$	1.770	85.390
$CaH_2 + NaNH_2$	1	$CaH_2 + NaNH_2 = CaNH + NaH + H_2$	0.409	39.463
	2	$CaH_2 + 2NaNH_2 = Na_2Ca(NH)_2 + 2H_2$	2.056	99.187
	3	$CaH_2 + 2NaNH_2 = CaNH + Na_2NH + 2H_2$	1.796	86.644
	4	Step 1: $CaH_2 + 2NaNH_2 = Ca(NH_2)_2 + 2NaH$	−0.458	
		Step 2A: $Ca(NH_2)_2 + 2NaH = CaNH + Na_2NH + 2H_2$	2.254	108.739
		Step 2B: $Ca(NH_2)_2 + 2NaH = Na_2Ca(NH)_2 + 2H_2$	2.514	121.282

experiment is at room temperature. From IR spectra [14] for the $2LiNH_2 + CaH_2$ composite, we can see that the $Ca(NH_2)_2$ phase does not appear during mechanical ball milling at ambient conditions. The absence of the intermediate $Ca(NH_2)_2$ phase at room temperature suggests that an energy barrier may exist that prevents the reaction, $CaH_2 + 2LiNH_2 \rightarrow Ca(NH_2)_2 + 2LiH$ from taking place. Even though formation of $Ca(NH_2)_2$–2LiH is thermodynamically most favorable, kinetics may play a role. The reaction will follow path 1 (note path 1 is thermodynamically preferred over path 2 and 3) if the energy barrier of the thermodynamically favored reaction in path 4 (step 1 in Table 2) is higher than the enthalpy of formation of path 1 (Table 2). However, once enough energy is provided by heating the mixture, the reaction with favorable thermodynamics will take over. The high temperature reaction will go through path 4 (Table 2) instead of path 1.

4.3. Mechanochemistry versus thermochemistry

Regardless of stoichiometry, high energy ball milling of MNH_2–CaH_2 (where M = Li or Na) mixtures leads to chemical reactions resulting in the formation of CaNH and alkali metal monohydride. In all cases, mechanochemical transformation occurs in a 1:1 molar ratio of components and proceeds as a one-step reaction according to a general schematic (7):

$$MNH_2 + CaH_2 \rightarrow CaNH + MH + H_2 \quad (7)$$

If the concentrations of starting materials are different from 1:1 molar, then the component that was in excess of equimolar stoichiometry remains in excess after the reaction described in (7) is completed. Formation of other calcium nitrides, amides or imides, such as Ca_3N_2, Ca_2N, Ca_2NH or $Ca(NH_2)_2$, $Li_2Ca(NH)_2$ was not observed, and it appears that CaNH is favored over other possible calcium compounds during mechanochemical treatment.

Compared to thermochemical transformations in MNH_2–CaH_2 systems, reactions induced by mechanical energy are different. For example, the dehydrogenation reaction of the $2LiNH_2$–CaH_2 mixture induced by heating and expressed as (4) is different from a reaction during the ball milling of the same system. Also, the stability of LiH and $LiNH_2$ in hydrogen desorption during mechanochemical processing and the formation of Li_2NH during heating makes the reaction mechanism and the final products different. In fact, formation of $Ca(NH_2)_2$ or $Li_2Ca(NH)_2$ compounds appears impossible using only mechanical energy since neither of them was observed even after ball milling for a long time.

The expected similarity of dehydrogenation processes in systems with lithium compared to their sodium analogues was also observed. In all reactions with lithium and sodium same types of products were obtained. The difference is only in the kinetics of the solid state reactions, which are always slower for sodium systems. Similar effect on kinetics when interchanging $LiNH_2$ and $NaNH_2$ was also observed in our previous work where we described mechanochemical transformations in $MAlH_4$–MNH_2 (M = Li, Na) systems [16].

To understand this difference in reaction rates, we note that during solid state transformations reaction kinetics is limited by diffusivity of atoms. Since both the atomic radius and mass of the Li atoms are much lower compared to Na, it is natural that mobility of lithium species is higher. This translates in the corresponding difference in the overall rates of mechanochemical reactions, which is always higher for lithium compounds. Following the same reasoning we predict that in the KNH_2:CaH_2 system phase transformation kinetics will be further suppressed.

From the thermodynamic calculations of the $LiNH_2$–CaH_2 system, presented in Table 2, it is clear that the most favorable reaction is between components in the 2:1 molar ratio. This is in a good agreement with the experimental thermochemical processes, described by Tokoyoda et al. [14]. The next possible transformation pathway is between the reactants taken in a 1:1 molar ratio. This is precisely the reaction that is observed during all mechanochemical transformations in the MNH_2–CaH_2 systems. In other words, the mechanochemical transformation pathway is the next most favorable thermodynamically.

Anomalies in the reaction pathways, observed during ball milling have recently been reviewed by Boldyrev [48]. Very high diffusion coefficients of atoms or ions constituting a solid phase is a distinctive feature of the mechanochemical solid state processes. To be distinguished from the ordinary diffusion determined by the concentration gradient, this type of diffusion is referred to as "deformational atomistic intermixing" or "ballistic diffusion". This diffusion can drive the system far from the equilibrium state and to a variety of stable or metastable configurations. Various structural defects generated during ball milling are also expected to affect the possible pathways of the reactions. Hence, nonequilibrium mechanochemical transformation pathways observed in the title systems add another dimension to transformations of complex hydride system that have relevance to the field of hydrogen storage materials.

5. Conclusions

Mechanochemical transformations of lithium and sodium amides with calcium hydride taken in 1:1, 1:2, 2:1 and 2:3 molar ratios, have been investigated. Formation of calcium imide, alkali metal monohydrides and gaseous hydrogen was observed for all investigated stoichiometries. In all cases, the overall mechanochemical transformations are equimolar and proceed as one-step reactions: $MNH_2 + CaH_2 \rightarrow CaNH + MH + H_2\uparrow$, where M = Li or Na. If the concentrations of starting materials are different from 1:1 molar, then the component whose concentration in the starting mixture was larger than equimolar remains in excess and does not transform up to 24 h of high energy ball milling. The reactions in lithium systems are faster compared to systems with sodium. Difference in hydrogen release kinetics can be related to differences in mobilities of lithium and sodium atoms, to differences in strength of ionic bonding of the imides and different thermodynamics. Total energies and enthalpies of formation for different reaction products during the dehydrogenation of CaH_2–MNH_2 mixtures were calculated. The reaction, $CaH_2 + 2MNH_2 \rightarrow Ca(NH_2)_2 + 2MH$ (M = Li, Na) was found to be exothermic. We conclude that there may exist two dehydrogenation path ways for CaH_2–MNH_2 with respect to experimental conditions: (I) mechanochemical transformation (7) driven by mechanical ball milling and (II) higher temperature two-step thermochemical transformations (path 4 in Table 2) driven by heating.

Acknowledgments

Support of this work by the Office of Basic Energy Science, Materials Sciences Division of the Office of Science of the US Department of Energy is acknowledged. Ames Laboratory is supported by the Office of Basic Energy Sciences, Materials Sciences Division of the Office of Science of the United States Department of Energy under contract No. DE-AC02–07CH11358 with Iowa State University. The computations used resources of the National Energy Research Scientific Computing Center, which is supported by the Office of Science of the US Department of Energy under Contract No. DE-AC02-05CH11231.

References

[1] P. Chen, Z. Xiong, J. Luo, J. Lin, K.L. Tan, Nature (London) 420 (2002) 302.

[2] T. Ichikawa, N. Hanada, S. Isobe, H.Y. Leng, H. Fujii, J. Alloys Compd. 404–406 (2005) 435.
[3] S. Isobe, T. Ichikawa, N. Hanada, H.Y. Leng, M. Fichtner, O. Fuhr, H. Fujii, J. Alloys Compd. 404–406 (2005) 439.
[4] W. Luo, J. Alloys Compd. 381 (2004) 284.
[5] Z. Xiong, G. Wu, J. Hu, P. Chen, Adv. Mater. 16 (2004) 1522.
[6] W. Luo, E. Ronnebro, J. Alloys Compd. 404–406 (2005) 392.
[7] W. Luo, S. Sickafoose, J. Alloys Compd. 407 (2006) 274.
[8] H. Leng, T. Ichikawa, S. Hino, T. Nakagawa, H. Fujii, J. Phys. Chem. B 109 (2005) 10744.
[9] T. Ichikawa, K. Tokoyoda, H. Leng, H. Fujii, J. Alloys Compd. 400 (2005) 245.
[10] Y. Chen, C.Z. Wu, P. Wang, H.M. Cheng, Int. J. Hydrogen Energy 31 (2006) 1236.
[11] R. Janot, J.-B. Eymery, J.-M. Tarascon, J. Power Sources 164 (2007) 496.
[12] S. Barison, F. Agresti, S.L. Russo, A. Maddalena, P. Palade, G. Principi, G. Torzo, J. Alloys Compd. 459 (2008) 343.
[13] G. Wu, Z. Xiong, T. Liu, J. Hu, P. Chen, Y. Feng, T.S. Wee, Inorg. Chem. 46 (2007) 517.
[14] K. Tokoyoda, S. Hino, T. Ichikawa, K. Okamoto, H. Fujii, J. Alloys Compd. 439 (2007) 337.
[15] Z. Xiong, G. Wu, J. Hu, P. Chen, J. Alloys Compd. 441 (2007) 152.
[16] O. Dolotko, H. Zhang, O. Ugurlu, J.W. Wiench, M. Pruski, L.S. Chumbley, V.K. Pecharsky, Acta Mater. 55 (2007) 3121.
[17] Y. Laurent, J. Lang, M.T. Le Bihan, Acta Crystallogr. B24 (1968) 494.
[18] O. Reckeweg, F.J. DiSalvo, Z. Anorg. Allg. Chem. 627 (2001) 371.
[19] E.T. Keve, A.C. Skapski, Inorg. Chem. 7 (1968) 1757.
[20] D.H. Gregory, A. Bowman, C.F. Baker, D.P. Weston, J. Mater. Chem. 10 (2000) 1635.
[21] C.F. Baker, M.G. Barker, A.J. Blake, Acta Crystallogr. E57 (2001) i6.
[22] O. Reckweg, F. DiSalvo, J. Solid State Sci. 4 (2002) 575.
[23] T. Sichla, H. Jacobs, Z. Anorg. Allg. Chem. 622 (1996) 2079.
[24] J.-F. Brice, J.-P. Motte, A. Courtois, J. Protas, J. Aubry, J. Solid State Chem. 17 (1976) 135.
[25] T. Sichla, H. Jacobs, Eur. J. Solid State Inorg. Chem. 32 (1995) 49.
[26] P. Bouclier, J. Portier, G. Turrell, J. Mol. Struct. 4 (1969) 1.
[27] J. Senker, H. Jacobs, M. Muller, W. Press, P. Muller, H.M. Mayer, R.M. Ibberson, J. Phys. Chem. B 102 (1998) 931.
[28] J. Senker, H. Jacobs, M. Muller, W. Press, H.M. Mayer, R.M. Ibberson, Z. Anorg. Allg. Chem. 625 (1999) 2025.
[29] W. Kohn, J. Sham, Phys. Rev. A140 (1965) A1133.
[30] Y. Wang, J.P. Perdew, Phys. Rev. B 44 (1991) 13298.
[31] G. Kresse, J. Furthmuller, Phys. Rev. B 54 (1996) 11169.
[32] P.E. Blochl, Phys. Rev. B 50 (1994) 17953.
[33] H. Jacobs, R. Juza, Z. Anorg. Allg. Chem. 391 (1972) 271.
[34] K. Miwa, N. Ohba, S. Towata, Y. Nakamori, S. Orimo, Phys. Rev. B 71 (2005) 195109.
[35] J.F. Herbst, L.G. Hector, Phys. Rev. B 72 (2005) 125120.
[36] Y. Song, Z.X. Guo, Phys. Rev. B 74 (2006) 195120.
[37] A. Zalkin, D.H. Templeton, J. Phys. Chem. B 60 (1956) 821.
[38] R.L. Lowton, M.O. Jones, W.I.F. David, S.R. Johnson, M. Sommariva, P.P. Edwards, J. Mater. Chem. 18 (2008) 2355.
[39] B. Wegner, R. Essmann, H. Jacobs, P. Fischer, J. Less-Commum. Met. 167 (1990) 81.
[40] N. Nagib, H. Jacobs, H. Kistrup, Atomkernenergie 33 (1979) 38.
[41] M.H. Sorby, Y. Nakamura, H.W. Brinks, T. Ichikawa, S. Hino, H. Fujii, B.C. Hauback, J. Alloys Compd. 428 (2007) 297.
[42] S. Bhattacharya, G. Wu, C. Ping, Y.P. Feng, G.P. Das, J. Phys. Chem. B 112 (2008) 11381.
[43] A.F. Andersen, A.J. Maeland, D. Slotfeldtellingsen, J. Solid State Chem. 20 (1977) 93.
[44] J.S. Tse, D.D. Klug, S. Desgreniers, J.S. Smith, R. Flacau, Z. Liu, J. Hu, N. Chen, D.T. Jiang, Phys. Rev. B 75 (2007) 134108.
[45] Y. Li, B. Li, T. Cui, Y. Li, L. Zhang, Y. Ma, G. Zou, J. Phys. Condens. Mater. 20 (2008) 045211.
[46] D.K. Smith, H.R. Leider, J. Appl. Crystallogr. 1 (1968) 246.
[47] A. Aguayo, D. Singh, J. Phys. Rev. B 69 (2004) 155103.
[48] V.V. Boldyrev, Russ. Chem. Rev. 75 (2006) 177.